FATIGUE BEHAVIOR OF ALUMINUM DECK FABRICATED BY FRICTION STIR WELDING

Ichiro OKURA[1], Nobuyasu HAGISAWA[2], Makoto NARUO[3] and Hitoshi TODA[4]

[1]Member of JSCE, Dr. Eng., Associate Professor, Department of Civil Engineering, Osaka University (2-1 Yamadaoka, Suita, Osaka 565-0871, Japan)
[2]Member of JSCE, M. Eng., Manager, Research & Development Center, Nippon Light Metal Co., Ltd. (1-34-1 Kambara-cho, Ihara-gun, Shizuoka 421-3291, Japan)
[3]Member of JSCE, M. Eng., Dept. of Bridge Design, Aichi Works, Ishikawajima-Harima Heavy Industries Co., Ltd. (11-1 Kitahama-cho, Chita, Aichi 478-8650, Japan)
[4]Manager, Bridge & Road Construction Division, Ishikawajima-Harima Heavy Industries Co., Ltd. (5-17 Hikari-cho, Kure, Hiroshima 737-8515, Japan)

An aluminum deck was fabricated by joining hollow extrusions with the friction stir welding (FSW). The purpose of this study is to make clear the fatigue behavior of the deck. First the material properties of the aluminum alloy used and the FSW region were investigated. Next a fatigue test was carried out for the deck, showing that a fatigue crack was initiated along the FSW-joining line of the top plate just under the load due to the plate-bending stress. Further fatigue tests were conducted for the beam-type specimens, revealing that where the supporting interval of the deck became large, a fatigue crack was caused perpendicularly to the FSW-joining line of the bottom plate by the membrane stress due to the global bending moment.

Key Words *: aluminum alloy, deck, friction stir welding, extrusion, fatigue*

1. INTRODUCTION

In Japan, the amendment of the design vehicle load from 196 kN to 245 kN in 1994 urges concrete slabs and girders of existing bridges to be reinforced. To cope with this issue, an idea of reducing the weight of the slab by replacing concrete slabs with aluminum decks is put forward. Furthermore, it is required that the roadway should be light for the suspension bridges with a longer span than that of the Akashi Strait Bridge. The use of aluminum decks will serve this purpose.

In the USA, there are many bridges to be repaired or strengthened because of their life-deficiency. As a solution they tried to replace existing concrete slabs with aluminum decks without changing foundations and supporting structures, and are giving actual results[1)].

The above background and incentive led to develop an aluminum deck using the friction stir welding. In this paper, the material properties of the region of the friction stir welding and the fatigue behavior of the aluminum deck were investigated by the static loading tests, fatigue tests and FE analysis.

2. FABRICATION OF TEST SPECIMENS

(1) Aluminum decks

Figure 1 shows a general idea of an aluminum deck on steel girders. The aluminum deck consists of the extrusions connected parallel. The longitudinal direction of the extrusions spans between

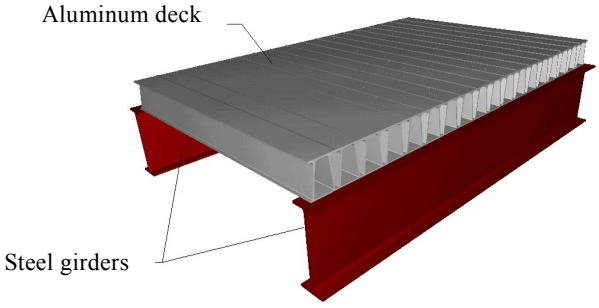

Fig.1 Aluminum deck on steel girders

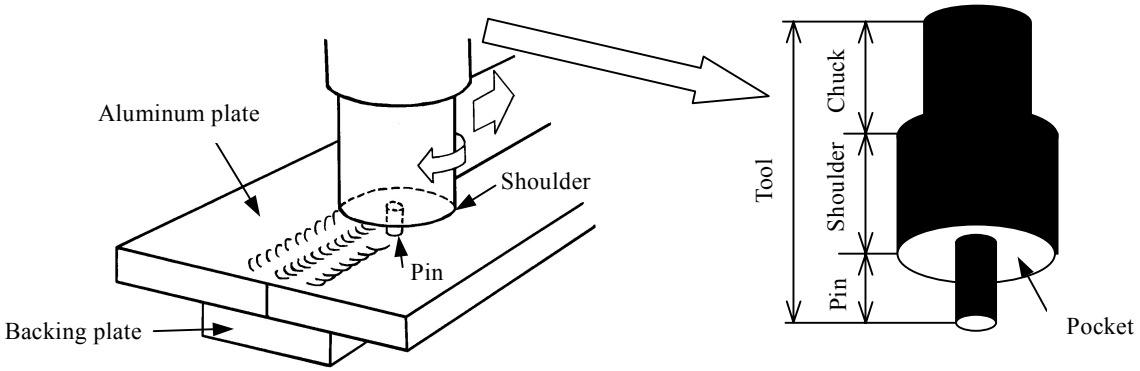

Fig.2 Concept of friction stir welding

main girders. In the past, we carried out FE analysis[2] of aluminum decks, and developed an aluminum deck whose extrusions were connected by caulking[3]. In this deck, however, the transfer of the bending moment was not adequate, though that of the shear force was adequate.

The MIG welding was an alternative to the caulking. However, fatigue cracks were reported to be initiated at the welds in steel plate decks[4]. So it was feared that the use of the MIG welding to fabricate aluminum decks would bring fatigue cracks at the welds.

Therefore, we adopted the friction stir welding (FSW) to connect extrusions[5)~8)]. It was expected that the fatigue strength of the connections by FSW would be higher than that by MIG welding, since FSW does not make any reinforcements at the connections.

(2) Friction stir welding (FSW)

FSW was invented in 1991 at the TWI, UK[9]. **Figure 2** shows the concept of FSW. Aluminum plates to be joined are butted together on a backing plate and are clamped so as not to move apart during joining. A rotating steel tool with a pin and a shoulder is plunged into the plates until the shoulder contacts the top surface. The butted surfaces are softened by frictional heating, dragged by the rotation of the tool, and stirred. The travel of the tool along the joining line makes the plates unite. FSW is a solid phase welding, because the stirred aluminum is not in a melting state.

The bottom of the shoulder of the tool is caved in to keep temporarily the stirred aluminum. The shape, called a pocket, is like a turned-over dish.

The section of the FSW joint consists of a stirred zone around the butted surfaces, plastic flow zones outside the stirred zone, and heat affected zones outside the plastic flow zones as shown in **Fig. 3**. Overlaps are formed on both sides of the joining line on the top surface.

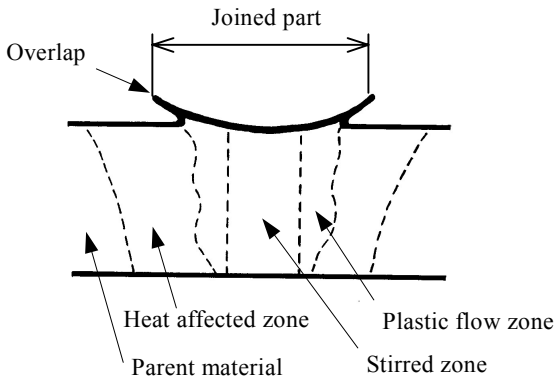

Fig.3 Constitution of friction stir welding joint

(3) Aluminum extrusions

Figure 4 presents the cross section of the extrusions for the aluminum deck. **Figures 4(a)** and **(b)** show the designed and measured dimensions of the cross section, respectively. The extrusions are 250 mm high, close to the thickness of commonly used reinforced concrete slabs. The width of 200 mm of the extrusions is in accordance with the size of an extruding die. The thickness of the extrusions is 10 mm from the requirement for the extruded length and the results of the past FE analysis[2], except 12 mm in thickness at the FSW joints from the considerations for the reduction in strength due to FSW. The webs of the extrusions are tilted in order to resist horizontal forces of vehicles.

The aluminum alloy used for the extrusions was A6N01-T5 specified in JIS H 4100. This material has good extrudability and high dimensional accuracy, which derives from the fact that rapid cooling is unnecessary due to low quench sensitivity.

(4) Fabrication method by FSW

The diameters of the shoulder and pin of the tool used for FSW were 25 mm and 6 mm, respectively. The rotational speed and the travel speed of

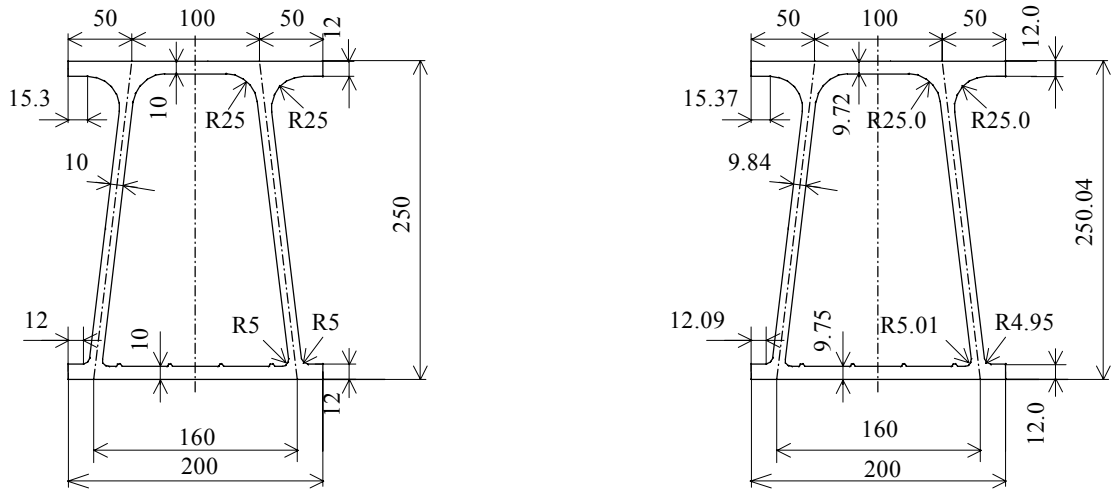

Fig.4 Cross section of extrusions

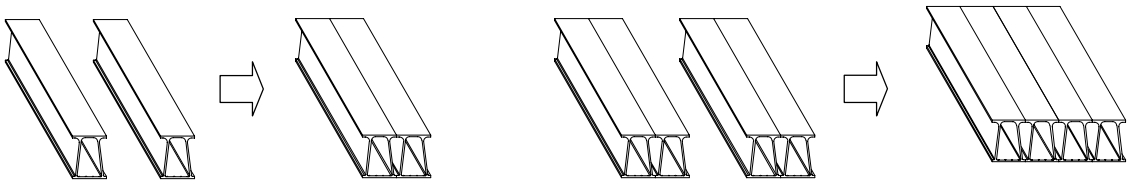

Fig.5 Fabrication of aluminum decks by friction stir welding

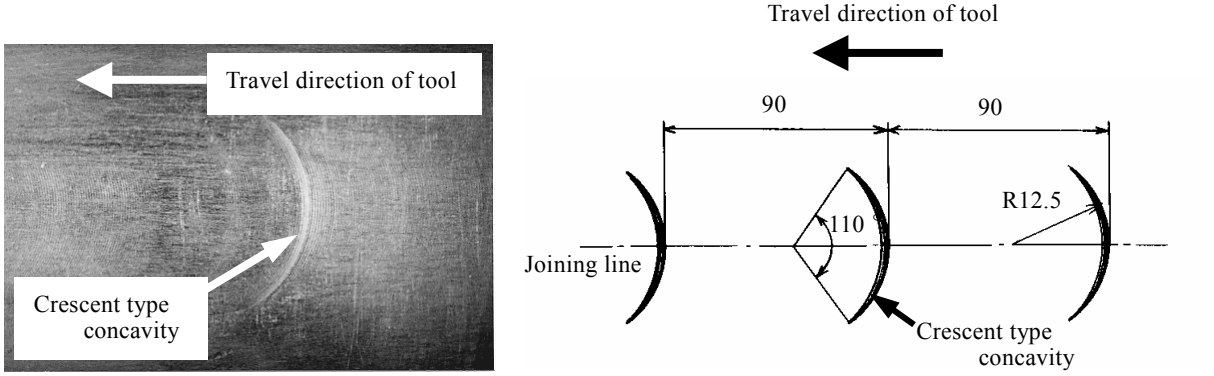

Fig.6 Crescent type concavity on the surface at FSW

the tool were 1200 rpm and 350 mm/minute, respectively. The thickness of the parts joined by FSW varied from 11.7 mm to 12.1 mm with the mean of 11.9 mm.

Figure 5 shows the fabrication method of the test specimens by FSW. First the two-extrusion panel is fabricated by joining one extrusion to another. Then the four-extrusion panel is formed by joining the two-extrusion panels to each other. Next the eight-extrusion panel is made by joining the four-extrusion panels to each other. This procedure continues till the prescribed panel is obtained. In FSW, the top and bottom flanges of the adjacent extrusions were butted to each other and a special device was inserted to keep the interval between the top and bottom flanges and to work as a backing plate. First the top flanges were joined and next the bottom flanges were joined after the panel was turned over. After the completion of the deck panel, the overlaps on both sides of the FSW were scraped off by a grinder.

As shown in **Fig. 6,** the crescent type concavities with depth of 0.2 to 0.3 mm are created at intervals of about 90 mm on the joined surface. In

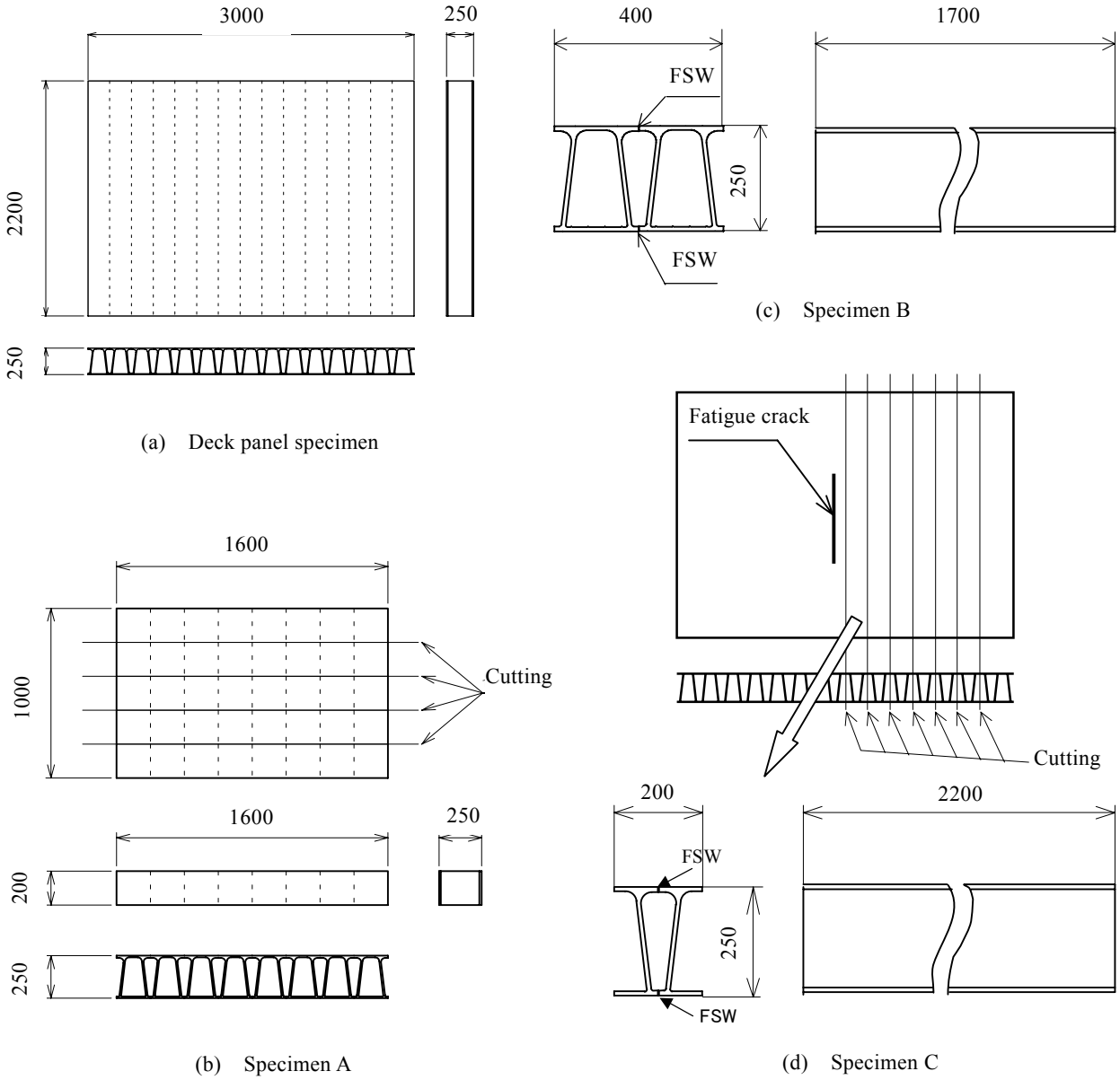

Fig.7 Specimens

the FSW process, the aluminum stirred by the pin is temporarily kept in the pocket shown in **Fig. 2**. When the volume of the pocket is too large, the softened aluminum is periodically discharged from the back of the shoulder of the moving tool, leading to the formation of the crescent type concavities. To shallow the pocket so that the aluminum more than the optimal volume can not stay in the pocket prevents those concavities.

Since the larger the panel, the larger the deformation of the panel becomes, the horizontal opening and vertical irregularity between the joining surfaces of the left and right panels increase. This raises the possibilities of the formation of the kissing bond such as shown in a macroscopic photograph of the cross section of the FSW in **Fig. 20**, at the tip of the pin of the tool.

(5) Specimens

As shown in **Fig. 7**, four kinds of test specimens were fabricated. As shown in **Fig. 7(a)**, the deck panel specimen consists of 15 extrusions 2200 mm long. As shown in **Fig. 7(b)**, cutting by a 200 mm width the panel of eight extrusions 1000 mm long makes the specimen A. In the specimen B, as shown in **Fig. 7(c)**, two extrusions 1700 mm long are joined. As shown in **Fig. 7(d)**, cutting the deck panel specimen in **Fig. 7(a)** after its fatigue test has been finished provides the specimen C.

Table 1 Chemical composition of extrusion of A6N01S-T5 alloy for deck

Item	Chemical composition (mass %)							
	Si	Fe	Cu	Mn	Mg	Cr	Zn	Ti
Measured data	0.51～0.53	0.16	0.08～0.09	0.14～0.15	0.69	0.01	0.01	0.02～0.03
JIS standard	0.04～0.9	≤0.35	≤0.35	≤0.50	0.40～0.8	≤0.30	≤0.25	≤0.10

Table 2 Mechanical properties of A6N01S-T5 alloy

Part		Tensile strength (MPa)	0.2% proof stress (MPa)	Proportional limit (MPa)	Young's modulus (GPa)	Poisson's ratio	Elongation (%)
Parent		270	246	221.3	70.5	0.31	7.9
FSW	FSW-L	218	128	83.7	69.1	0.34	29.8
	FSW-T	217	111	56.7	69.3	0.33	

3. MATERIAL PROPERTIES

Various types of test pieces were made from the specimen B to obtain the material properties of the parent material and the FSW. The measured chemical composition of the aluminum alloy used for the specimens is listed in **Table 1** together with the values specified in JIS H 4100.

(1) Width of heat affected zone

The hardness on the cross section of the FSW was measured to know the width of the heat affected zone (HAZ) of the FSW. **Figure 8** presents the distribution of the Vickers hardness on the cross section of the FSW of the top flange. The hardness of the bottom flange were similar to this. In **Fig. 8**, the hardness decreases for a 20 mm distance in each direction from the center of the FSW joint. The HAZ in MIG welding usually extends a 25 mm distance in each direction from the center of the welds[10]. Accordingly the width of the HAZ in FSW is smaller than that in MIG welding.

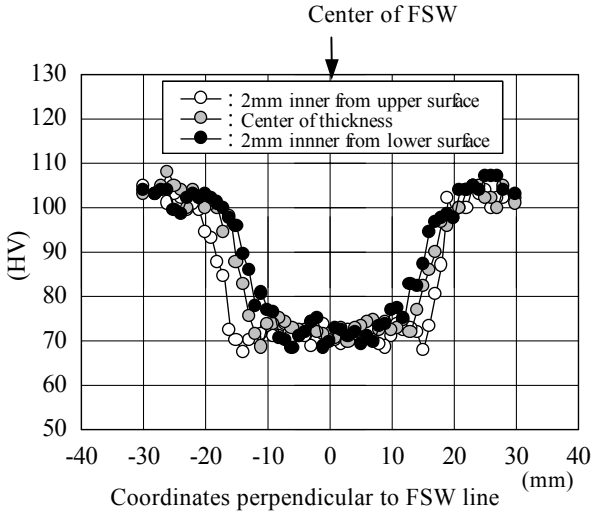

Fig.8 Vickers hardness on the section of FSW of top flange

(2) Tensile properties

Table 2 lists the results of the tensile tests for the parent material and the FSW. The size of the test pieces accorded with 14B in JIS Z 2201. Strain gauges with gauge length of 5 mm were used to determine the 0.2 % proof stress.

Seven test pieces for the parent material were cut out in the longitudinal direction of the extrusions. Six and seven test pieces for the FSW were cut out in the longitudinal direction (FSW-L) and in the transverse direction (FSW-T) of the specimen B, respectively.

The ratios of the material properties of FSW-L to those of the parent material were 0.81, 0.52 and 0.38 on the tensile strength, the 0.2 % proof stress and the proportional limit, respectively. Similarly the ratios of the FSW-T to the parent material were 0.80, 0.45 and 0.26, respectively. The 0.2 % proof stress and the proportional limit fell largely compared with the tensile strength. There was a large difference in the proportional limit between the FSW-L and -T. All the test pieces of FSW-T broke at the heat affected zone shown in **Fig. 3**.

The ratios of the MIG welds to the parent material for the tensile strength and the 0.2 % proof stress were 0.74 and 0.56, respectively[10]. The fall in the tensile strength in the FSW was smaller than that in the MIG welds. The decrease in the 0.2 % proof stress in the FSW, however, was larger than that in the MIG welds.

(3) Residual stresses

Figure 9 shows the residual stresses on the surfaces on the insertion side of the pin of the tool, in the longitudinal and transverse directions to the FSW-joining line. Biaxial strain gauges with five elements were glued on the outer surfaces of the

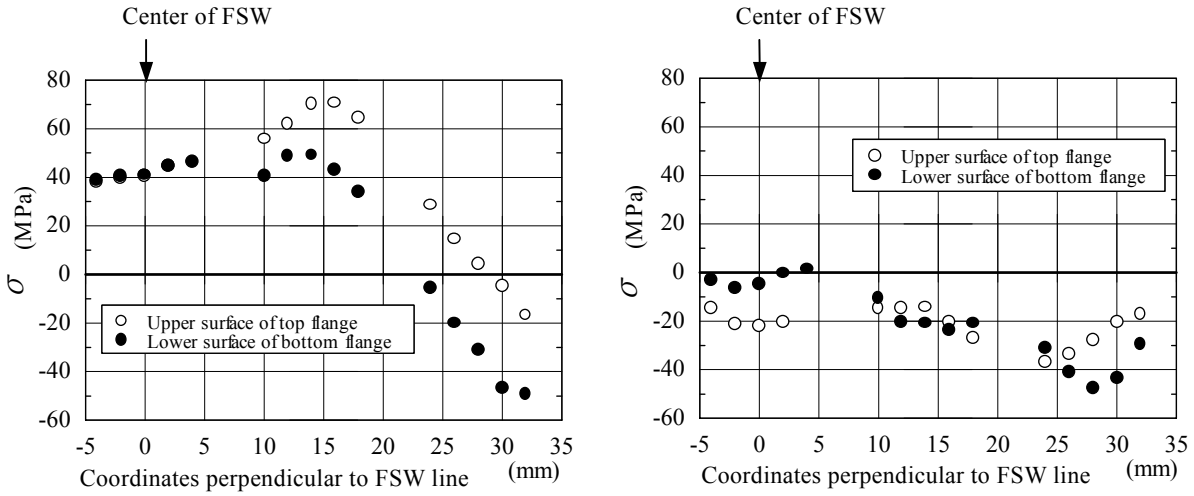

(a) Residual stresses parallel to FSW line (b) Residual stresses perpendicular to FSW line

Fig.9 Residual stresses at FSW on the outer surfaces

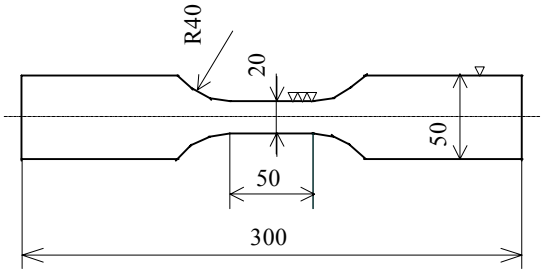

Fig.10 Fatigue test piece

Table 3 Values of log c, m and ξ_N

Part	R	m	log c	ξ_N
Parent	–1	7.66	23.9	0.073
	0.1	6.58	20.3	0.214
	0.5	7.31	20.5	0.366
FSW-T	–1	8.74	25.9	0.148
	0.1	6.84	20.1	0.133
	0.5	6.70	18.8	0.525
FSW-L	0.1	3.58	13.6	0.439
	0.5	4.91	15.5	0.163

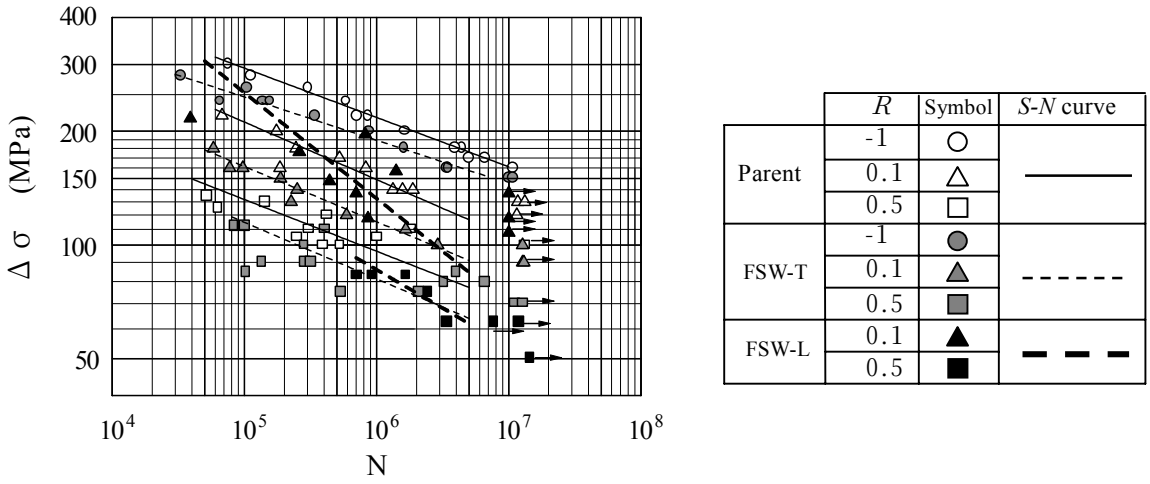

Fig.11 *S-N* curve

top and bottom flanges at the middle in the longitudinal direction of the specimen B. Cutting the specimen into small pieces releases the residual strains, and the released strains were measured by the strain gauges. The residual stresses on the surfaces on the insertion side of the pin of the tool are tensile and compressive in the parallel and perpendicular directions to the joining line, respectively.

(4) Fatigue properties

Figure 11 presents the results of the fatigue tests of the pieces in **Fig. 10**. An axial load was applied to the test pieces. The test pieces for the parent material were cut out from the extrusions in the longitudinal direction. Those for the FSW were cut out in the longitudinal direction (FSW-L) and in the transverse direction (FSW-T) of the specimen B. The crescent type concavities mentioned in 2(4) were avoided on the part 20 mm wide in the

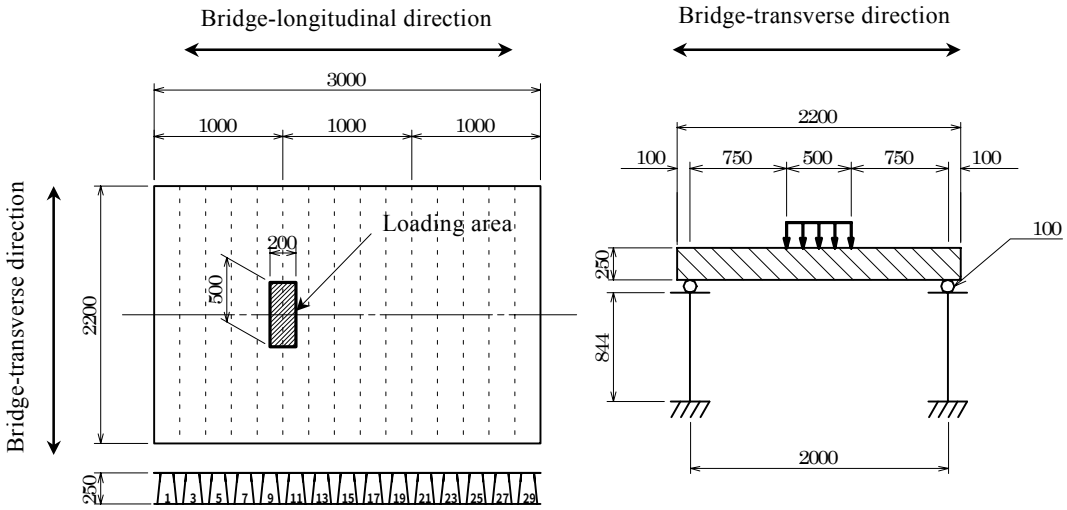

Fig.12 Static loading test of aluminum deck

middle of the test pieces for the FSW. A total of 34 pieces of FSW-T failed, 23 at the heat affected zone and 11 at the stirred or plastic flow zone.

As shown in **Fig. 11**, at each stress ratio, the fatigue strength decreases in order of the parent material, FSW-L and FSW-T. The *S-N* curves in **Fig.11** are given in the following form:

$$\log N = \log c - m \log(\Delta \sigma) \qquad (1)$$

where N is the number of cycles to failure, c and m are coefficients, and $\Delta\sigma$ is the stress range.

Table 3 lists the values of m, $\log c$ and the standard deviation ξ_N of $\log N$ about the arbitrary $\log(\Delta\sigma)$ determined by the least squares method, treating $\log(\Delta\sigma)$ and $\log N$ as an independent and dependent variables, respectively. The slopes of the *S-N* curves of the parent material and FSW-T are close to each other. However, the slopes of the FSW-L are different from these. As seen from **Fig. 11**, the results of the FSW-L are few in the low cycle region. Accordingly it is estimated that if the number of the results of the FSW-L increases in the low cycle region, the slopes of the FSW-L will approach the ones of the parent material and FSW-T.

4. FATIGUE TEST AND FE ANALYSIS OF ALUMINUM DECK

(1) Static loading test

Figure 12 shows the outline of the static loading test of the deck panel specimen shown in **Fig. 7(a)**. Hereafter, the upper and lower flanges of the joined extrusions are called the top and bottom plates, respectively. The deck is put on the steel

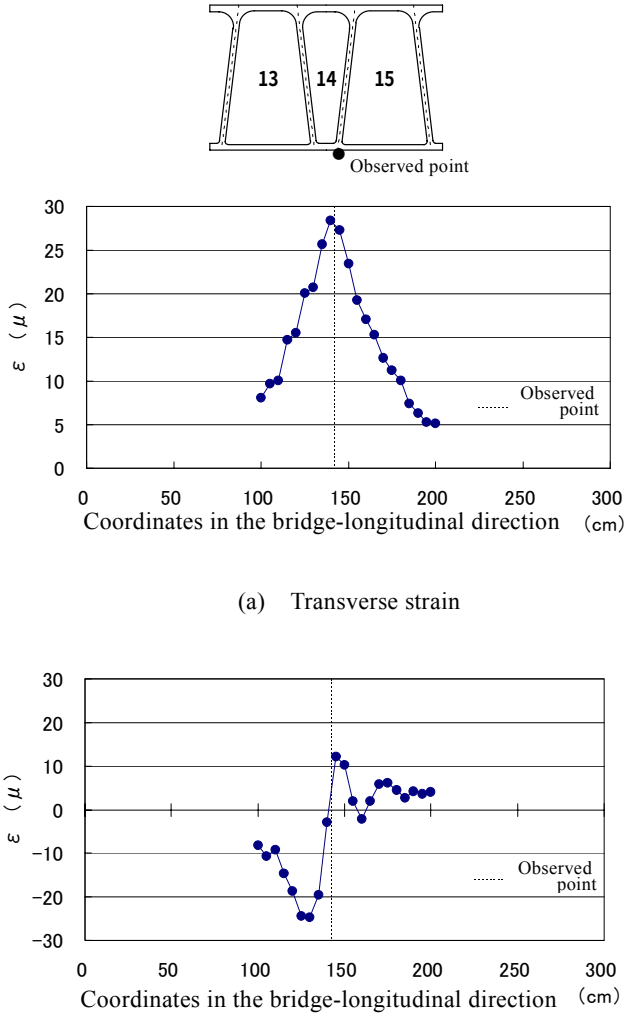

Fig.13 Influence lines of strains on lower surface of bottom plate

round bars 100 mm in diameter that are laid on steel girders 844 mm high and 4000 mm long. The supporting interval of the deck is 2000 mm. A load is applied to the top plate through a hard rubber plate (200×500×15 mm). The shape of 200×500 mm is the same as the loading area of the design wheel load of a truck specified in the Japanese Specifications for Highway Bridges[11]. The load was applied statically after moving the deck at every 50 mm interval in the bridge-longitudinal direction.

Figure 13 presents the influence lines of the strains in the bridge-transverse and -longitudinal directions obtained from the static test. The results are corresponding to the load of 9.8 kN. For the move of the load, the stress in the bridge-longitudinal direction alternates positive and negative, but the stress in the bridge-transverse direction does not.

(2) Fatigue test

Figure 14 gives the location and magnitude of the fatigue load. In the loading case 1, the load is on the cell where the FSW does not exist, and in the loading cases 2 and 3, it is on the cell where the FSW exists. In each of the loading cases, the load is located in the middle between the two steel girders, as shown in the right-hand figure in **Fig. 12**. Since the bottom plate of the deck was not perfectly flat, some gap occurred between the bottom plate and the steel round bars, and the bottom plate hit the bars during the repetition of the load below 49.0 kN. Hence, 49.0 kN was accepted for the lower load.

In the loading case 1, the fatigue test was finished at two million cycles, since neither the change of the deflection range, the strain range nor the initiation of fatigue cracks was recognized.

In the loading case 2, the strain range on the FSW-joining line of the top plate varied at one million cycles. The fatigue test, however, was continued until two million cycles, since neither the change of the deflection range nor the initiation of fatigue cracks was recognized.

In the loading case 3, the strain range on the FSW-joining line of the top plate began to vary at 1.02×10^5 cycles. The fatigue test, however, was continued until one million cycles, since the deflection range did not change. Taking off the rubber plate led to find a fatigue crack 48 cm long along the FSW-joining line of the top plate at that time. The fatigue crack already penetrated the top plate, since the dye penetrant spread on the upper surface appeared on the lower surface. The fatigue test, however, was continued until two million cycles, since the deflection range did not change. The fatigue crack grew 62 cm long. Hereafter this crack is called the type 1 crack.

Case	Lower load (kN)	Upper load (kN)	Load range (kN)
1	49.0	186.3	137.3
2	49.0	186.3	137.3
3	49.0	268.7	219.7

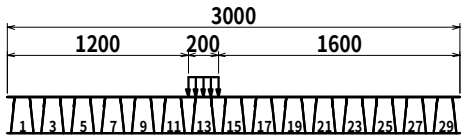

(a) Case 1

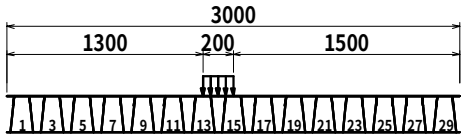

(b) Cases 2 and 3

Fig.14 Location and magnitude of fatigue load

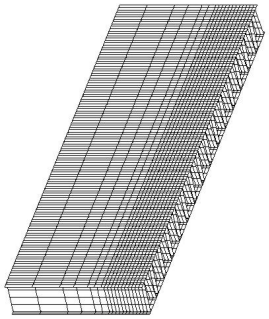

Fig.15 Mesh division

Since the crack propagates along the FSW-joining line, the type 1 crack is produced by the stress in the bridge-longitudinal direction.

(3) FE analysis

To make clear the structural behavior of the deck and the characteristics of the stress to produce the type 1 crack, the FE analysis was carried out, using MARC[12], an FEM software. The mesh division of the analytical model is given in **Fig. 15**. The finite elements used are an eight-node thick shell element (Element type 22 in MARC).

Since the deck is symmetrical, its half is divided into elements. The bottom plate on the left side in **Fig. 15** is supported vertically and the boundary conditions of symmetry are imposed on the right side. The uniformly distributed load was divided

into concentrated loads, depending on the area. Then the concentrated loads were applied to the loading area of the cases 2 and 3 in **Fig. 14**. The computation was done in the elastic range with Young's modulus of 70.5GPa and Poisson's ratio of 0.31.

Figure 16 provides the stress distributions of the top and bottom plates in the bridge-transverse direction just under the load. The results are corresponding to the load of 137.3 kN. The horizontal axis is the coordinates in the bridge-transverse direction with the origin of the supporting point. The experimental results agree well with the ones of the FE analysis.

The stress in the bridge-transverse direction in **Fig. 16(a)** is a plate-bending stress on the top plate just under the load. Except this area, it is a membrane stress on the top and bottom plates.

As shown in **Fig. 16(b)**, the stress in the bridge-longitudinal direction is a plate-bending stress on the top and bottom plates. The plate-bending stress on the top plate is very high within the loading area, and it decreases rapidly outside the loading area. Accordingly this stress is produced by the local out-of-plane deformation of the top plate just under the load, and it has no relation to the size of the supporting interval of the deck. This means that the type 1 crack is initiated irrelevant to the size of the supporting interval of the deck. Since the plate-bending stress on the top plate is compressive on the upper surface and tensile on the lower surface, the type 1 crack is initiated on the lower surface and propagates toward the upper surface.

Figure 17 shows the stress distributions on the lower surface of the bottom plate in the bridge-longitudinal direction just under the load. The results are corresponding to the load of 137.3 kN. The horizontal axis is the coordinates in the bridge-longitudinal direction with the origin of the upper side in **Fig. 15**. The experimental results are close to the ones of the FE analysis. Both of the transverse and longitudinal stresses are observed obviously for a 500 mm distance on each side from the loading point. This means that the aluminum deck is a structure in which a load is supported in the limited area around the location of the load.

5. FATIGUE STRENGTH OF TYPE 1 CRACK

To obtain the fatigue strength of the type 1 crack, the fatigue tests were carried out using the

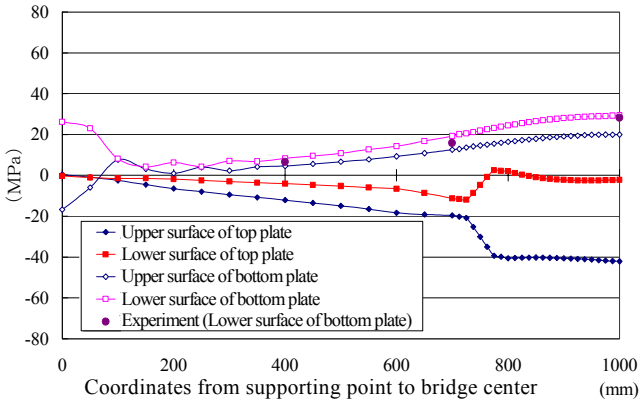

(a) Transverse stress

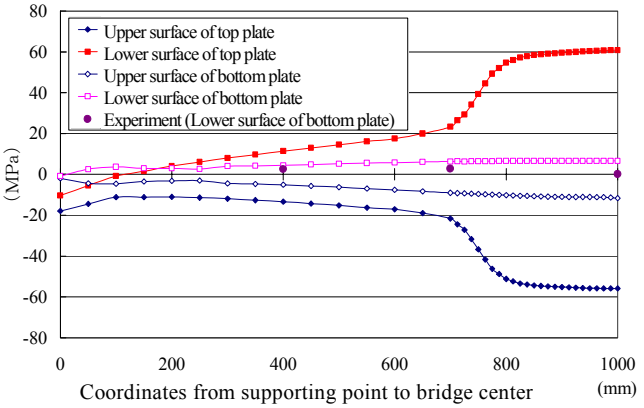

(b) Longitudinal stress

Fig.16 Stress distributions in the bridge-transverse direction just under the load

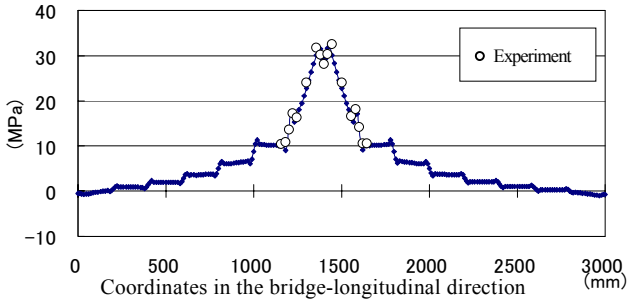

(a) Transverse stress

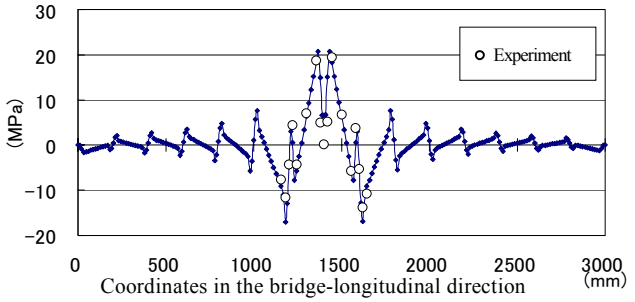

(b) Longitudinal stress

Fig.17 Stress distributions in the bridge-longitudinal direction on lower surface of bottom plate just under the load

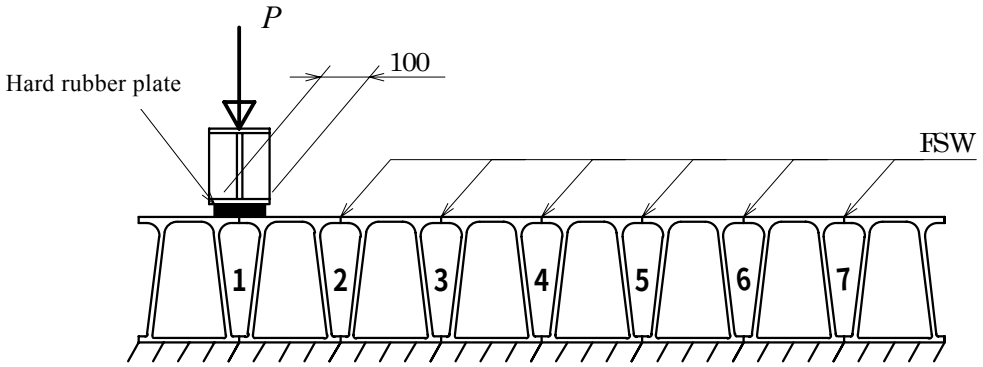

Fig.18 Fatigue test of specimen A

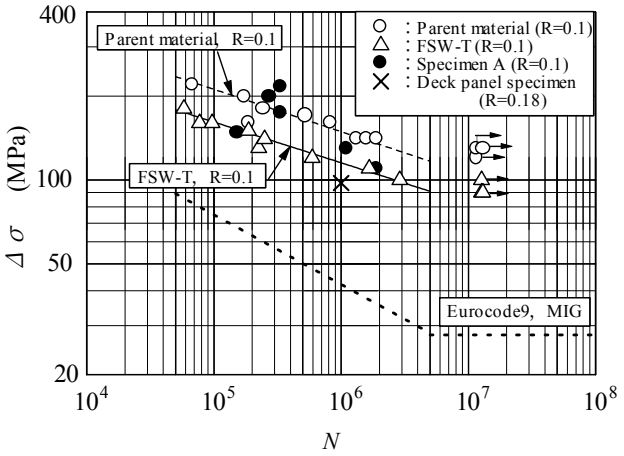

Fig.19 Fatigue strength of type 1 crack

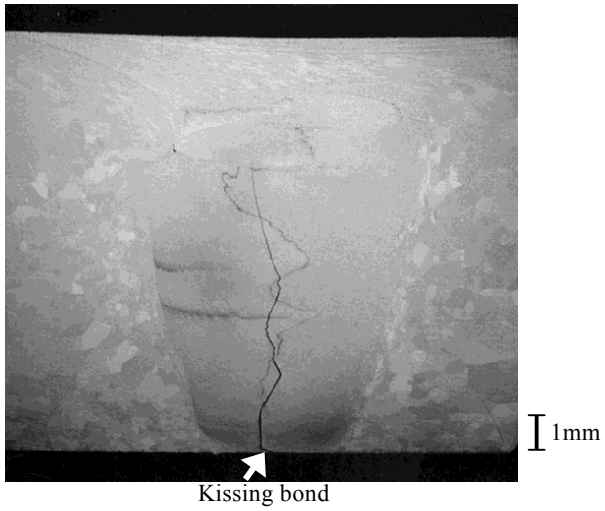

Fig.20 Macroscopic photograph of the section of FSW of specimen A after the tests

specimen A. As shown in **Fig. 18**, the bottom plate of the specimen is fixed on a test floor, and a load is applied to the FSW of the top plate through a hard rubber plate (250×100×15 mm). After an FSW joint broke due to fatigue, the load was moved to the neighboring FSW joint, followed by the fatigue test. We confirmed that the load on an FSW joint did not induce such a strain as to affect the fatigue strength of the neighboring one.

Figure 19 presents the results of the fatigue tests. The stress ratio is 0.1. $\Delta\sigma$ is the stress range at the FSW on the lower surface of the top plate, calculated from the measured strains. N is the number of cycles to failure. In this figure, the results of the tensile-test type pieces of the stress ratio of 0.1 for the parent material and the FSW-T in **Fig. 11** and the design *S-N* curve for the MIG welds specified in Eurocode 9[13] are also given. The design *S-N* curve is for the butt welds whose welding line is perpendicular to the direction of stress and for the conditions of non-grinding.

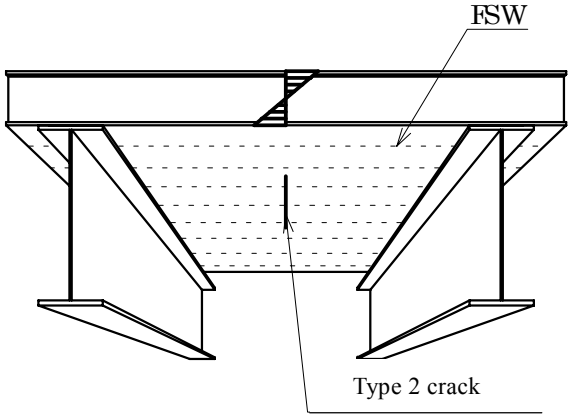

Fig.21 Type 2 crack

As seen from **Fig. 19**, the fatigue strength of the FSW of the specimen A is much higher than that of the MIG welds. The fatigue strength of the FSW of the specimen A is generally higher than that of the FSW-T of the tensile-test type specimens, but it scatters widely. The fatigue test of the FSW of the specimen A was performed in bending.

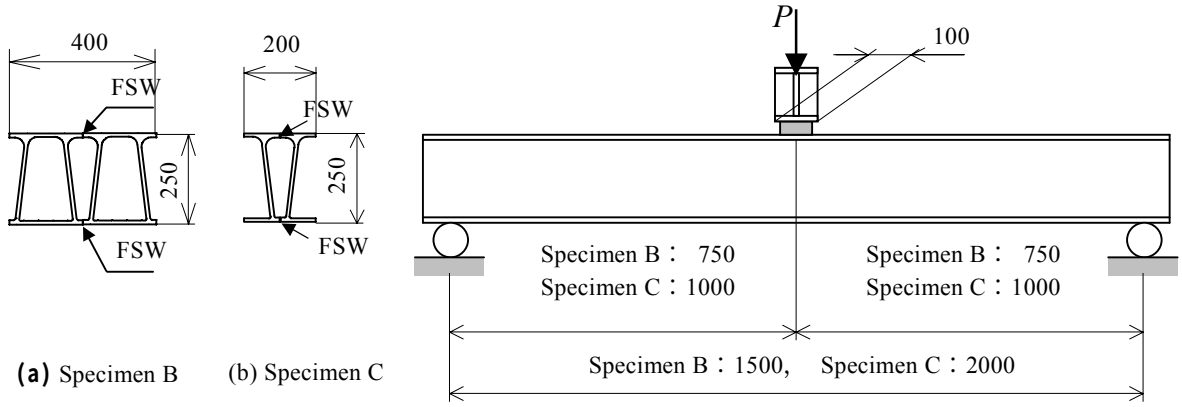

Fig.22 Fatigue tests of specimen B and C

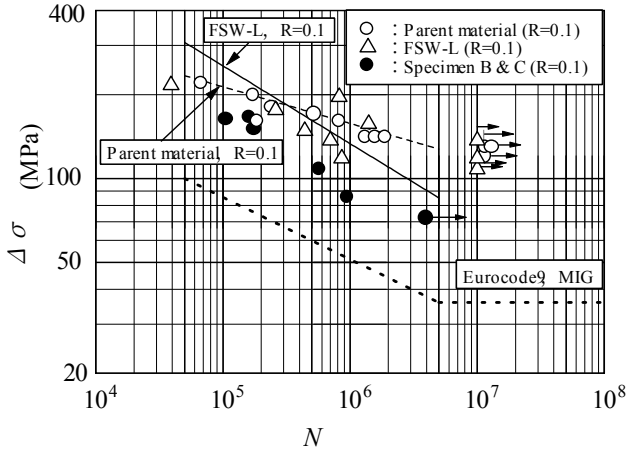

Fig.23 Fatigue strength of type 2 crack

Generally the fatigue strength in bending is higher than that in tension. As mentioned in 2(4), the larger the panel, the higher the possibilities of the formation of the kissing bond at the tip of the pin of the tool become. This is the reason the scatter of the fatigue strength of the FSW of the specimen A is enlarged. After the fatigue test, as shown in the macroscopic photograph in **Fig. 20**, the kissing bond 0.25 mm deep is observed at the FSW at the middle of the specimen A.

The fatigue strength of the deck panel specimen is provided in **Fig. 19** as well. In the loading case 3, the length of the fatigue crack at the FSW on the top plate was 48 cm at one million cycles. Since this length was almost the same as the loading width of 500 mm, one million cycles were taken as the fatigue life of the deck panel specimen to be compared with that of the specimen A. The stress range is the one in the bridge-longitudinal direction on the lower surface of the top plate just under the load, and its magnitude is 97.4 MPa. The value of 97.4 MPa was given by the FE analysis mentioned in 4(3), which was corresponding to the load range of 219.7 kN of the loading case 3.

The stress ratio of the deck panel specimen is higher than that of the specimen A. Even though we consider this, the fatigue strength of the deck panel specimen may be lower than that of the specimen A. The kissing bond 0.5 mm deep was observed at the FSW joint of the deck panel specimen where the type 1 fatigue crack was initiated. This is larger than the kissing bond 0.25 mm deep of the specimen A. This will be the reason the fatigue strength of the deck panel specimen is somewhat lower than that of the specimen A.

6. FATIGUE STRENGTH OF TYPE 2 CRACK

Since the supporting interval of the deck panel specimen was short as 2000 mm, fatigue cracks would not have been caused on the bottom plate. As shown in **Fig. 21**, as the supporting interval becomes large, the global bridge-transverse bending moment increases, and a fatigue crack will be produced at the FSW of the bottom plate in the bridge-longitudinal direction. Hereafter this crack is called the type 2 crack. To obtain the fatigue strength of this crack, the fatigue tests were carried out using the specimens B and C.

As shown in **Fig. 22**, both ends of the specimens are supported with rollers and the fatigue load is applied to the 100 mm width at the span center. The supporting intervals of the specimens B and C are 1500 mm and 2000 mm, respectively. By the strain values measured on the deck panel specimen and the ones by the FE analysis in 4(3), it was confirmed that such a strain as to affect the fatigue strength of the specimen C was not induced in the fatigue test of the deck panel specimen.

The type 2 crack was initiated at the FSW on the lower surface of the bottom plate. It propa-

gated across the specimen, and the specimen broke into two pieces due to brittle fracture. The crack started at the concavity mentioned in 2(4) in three out of the five broken specimens.

Figure 23 presents the results of the fatigue test. The stress ratio is 0.1. $\Delta\sigma$ is the stress range at the crack initiation point of the bottom plate, estimated by the interpolation of the measured strains on both sides of the crack. N is the number of cycles to failure. In this figure, the results of the tensile-test type specimens of the stress ratio of 0.1 for the parent material and the FSW-L in **Fig. 11** and the design *S-N* curve for the MIG welds specified in Eurocode 9[13] are also provided. The design *S-N* curve is for the butt welds whose welding line is parallel to the direction of stress and for the conditions of non-grinding.

As seen from **Fig. 23**, the fatigue strength of the specimens B and C is much higher than that of the MIG welds. However it is lower than that of the FSW-L of the tensile-test type specimens. This is due to the concavity left at the FSW and the fact that as was mentioned in 3(3), the residual stress in the direction of the FSW-joining line is tensile.

7. CONCLUSIONS

In this study, the fatigue behavior of an aluminum deck fabricated by FSW was investigated by the material tests, static loading tests, fatigue tests and FE analysis of the deck panel specimen and three kinds of specimens cutting out from the deck panel specimen. The main results are as follows:

(1) The heat affected zone of the FSW extends a distance of 20 mm in each direction from the center of the FSW.
(2) In the FSW, the decreases in the 0.2 % proof stress and the proportional limit are large compared with that of the tensile strength.
(3) The residual stresses on the surfaces on the insertion of the pin of the tool are tensile and compressive in the longitudinal and transverse directions to the joining line, respectively.
(4) Using tensile-test type pieces, *S-N* curves are given for the parent material and the FSW in the longitudinal and transverse directions to the joining line.
(5) In the aluminum deck, the stress in the bridge-longitudinal direction alternates positive and negative for the move of a load, but the stress in the bridge-transverse direction does not.
(6) The aluminum deck is a structure in which a load is supported in the limited area around the load.
(7) The type 1 fatigue crack is initiated along the FSW-joining line of the top plate of the deck. This crack is due to the plate-bending stress in the bridge-longitudinal direction. This stress is produced by the local out-of-plane deformation of the top plate just under the load, and it has no relation to the size of the supporting interval of the deck, that is, the initiation of the type 1 crack is irrelevant to the size of the supporting interval of the deck. The fatigue strength of the type 1 crack is much higher than that of the butt welds by MIG specified in Eurocode 9 whose welding line is perpendicular to the direction of stress and that are in the conditions of non-grinding.
(8) Where the supporting interval of the deck becomes large, the type 2 crack is initiated at the FSW of the bottom plate in the bridge-longitudinal direction. This crack is due to the membrane stress in the bridge-transverse direction, produced by the global bending moment. The fatigue strength of the type 2 crack is much higher than that of the butt welds by MIG specified in Eurocode 9 whose welding line is parallel to the direction of stress and that are in the conditions of non-grinding.

ACKNOWLEDGMENT: This paper stands on the research accomplished in the Aluminum Deck Committee which was held in the Japan Aluminum Association in 1999 with the subsidies from the Agency of Industrial Science and Technology, Japan. The writers would like to thank the committee members for their valuable comments. Thanks are also due to Mr. G. L. Vigh, an exchange student of Osaka University from Budapest University of Technology and Economics, Hungary and Mr. T. Nakahara, a graduate student of Osaka University for their assists in carrying out the fatigue tests of the specimens B and C.

REFERENCES

1) Civil Engineering: New Aluminum Decks Cut Loads, Add Life, *ASCE,* p. 2, Aug., 1996.
2) Japan Aluminium Federation: Review on Aluminum Civil Structures, 1997 (In Japanese).
3) Japan Aluminium Federation: Aluminum Deck Fabri-

cated by Caulking, 1998 (In Japanese).
4) Okura, I.: *Fatigue in Steel Bridges*, pp.336-339, Toyo Publisher, 1994 (In Japanese).
5) Japan Aluminium Association: Basic Data on Aluminum Decks, Mar., 2000 (In Japanese).
6) Okura, I.: Application and Prospect of Aluminum to Bridges, *Japan Institute of Light Metals, 59th Symposium*, pp. 19-31, 2000 (In Japanese).
7) Okura, I., Naruo, M., Vigh, L.G., Hagisawa, N. and Toda, H.: Mechanical and structural properties of aluminum decks fabricated by friction stir welding, *JECE, Proceedings of the 2nd Symposium on Decks of Highway Bridges*, pp.131-136, 2000 (In Japanese).
8) Okura, I., Naruo, M., Vigh, L.G., Hagisawa, N. and Toda, H.: Fatigue of aluminum deck fabricated by friction stir welding, *Proceedings of 8th International Conference on Joints in Aluminum, Munich, Germany*, pp. 4.1.1-4.1.12, 2001.
9) http://www.twi.co.uk/bestprac/datashts/fswintro.html
10) Japan Aluminium Association: *Recommendations for Design and Fabrication of Aluminum Alloy Structures-1st Draft*, Dec. 1998 (In Japanese).
11) Japan Road Association: *Japanese Specifications for Highway Bridges*, Part 2 Steel Bridges, 1996 (In Japanese).
12) Marc Analysis Research Corporation: MARC-K.7, 1997.
13) Eurocode 9: *Design of Aluminum Structures, Part 2 Structures Susceptible to Fatigue*, prENV 1999-2, 1997.

(Received May 16, 2002)